Triggering the Continuous Growth of Graphene Toward Millimeter-Sized Grains

Tianru Wu, Guqiao Ding, Honglie Shen, Haomin Wang, Lei Sun, Da Jiang, Xiaoming Xie,* and Mianheng Jiang*

A simple but efficient strategy to synthesize millimeter-sized graphene single crystal grains by regulating the supply of reactants in the chemical vapor deposition (CVD) process is demonstrated. Polystyrene is used as a carbon source. Pulse heating on the carbon source is utilized to minimize the nucleation density of graphene on copper foil, while a gradual increase in the temperature of the carbon source and the flow rate of hydrogen is adapted to drive the continuous growth of the graphene grains. As a result, the nucleation density of graphene grain can be controlled to as low as ≈100 nuclei/cm^2, and a single crystal grain can grow up to dimensions of ≈1.2 mm. Raman spectroscopy, transmission electron microscopy (TEM), and electrical-transport measurements show that the graphene grains obtained are of high quality. The strategy presented provides very good controllability and enables the possibility of large graphene single crystals, which is of vital importance for practical applications.

1. Introduction

Graphene, a monolayer of sp^2 carbon atoms, has been attracting great interest as an ideal two dimensional (2D) crystalline material.[1] Its 2D nature and high carrier mobility provide a great platform for exploration of high performance electronics. Fabrication techniques for wafer scale graphene are already available. However, graphene in wafer scale differs from normal silicon as it is mainly polycrystalline with typical grain size in the range of micrometers or tens of micrometers.[2–4] The synthesis of a continuous graphene film with large grain size is still a great challenge.[5,6]

Synthesis of graphene with millimeter-sized grains was demonstrated by several groups. Wang et al.[7] realized the growth of rectangular-shaped graphene domain on copper foil with dimension of about 0.4 mm based on ambient pressure CVD (APCVD), with a growth temperature of 1030 °C. They found that pre-annealing of Cu foil could remarkably reduce the graphene nucleation density. Li et al.[8] succeeded in making graphene domain with lateral size of 0.5 mm, via low pressure chemical vapor deposition (LPCVD) process by using methane as a precursor at 1035 °C. The graphene grains obtained are dendrite-shaped, which may contain single-crystal-subgrains. They found that graphene growth rate gradually slows down with the increase of growth time, due to reduced copper surface exposure. Later, Gao et al.[9] achieved millimeter-sized grain in hexagonal shape on Pt foil. It took more than 3 hours to grow ~1 mm single-crystal grains. Although the above experiments demonstrated the growth of large grains, none of them gave a clear picture about the growth dynamics.

In this manuscript, we demonstrated a simple but efficient strategy to synthesis millimeter-sized graphene grains by APCVD. The key is to maintain low nucleation rate and to provide continuous drive for graphene growth. Nucleation density as low as ~100 nuclei/cm^2 was achieved by optimizing process parameters on copper substrate subjected to fine polishing and pre-annealing. A continuous increase of carbon supply and the total gas flow rate drive the continuous graphene growth. Single crystal graphene domain of 1.2 mm in size was successfully synthesized, which is so far the largest one reported on Cu substrate.

2. Results and Discussion

Polystyrene was chosen as the carbon source because of its relative weak C-H bonds and low decomposition temperature compared to the widely used gaseous sources.. The C-H bond in polystyrene is comparatively weak, with a bond energy in between 292–305 kJ/mol, much lower than that in typical gaseous carbon precursors such as methane (410 kJ/mol), ethylene (443 kJ/mol) and ethyne (506 kJ/mol).[10] We heated the polystyrene to a temperature lower than 280 °C (defined as T_p hereafter). The products decomposed from polystyrene were analyzed by means of gas chromatography and mass

T. R. Wu, Prof. H. L. Shen, L. Sun
College of Materials Science & Technology
Nanjing University of Aeronautics & Astronautics
Nanjing, 211100, China
E-mail: hlshen@nuaa.edu.cn
Dr. G. Q. Ding, Prof. H. M. Wang, Prof. D. Jiang, Prof. X. M. Xie, Prof. M. H. Jiang
State Key Laboratory of Functional Materials for Informatics
Shanghai Institute of Microsystem and Information Technology
Chinese Academy of Sciences
865 Changning Road, Shanghai 200050,
People's Republic of China
E-mail: xmxie@mail.sim.ac.cn

DOI: 10.1002/adfm.201201577

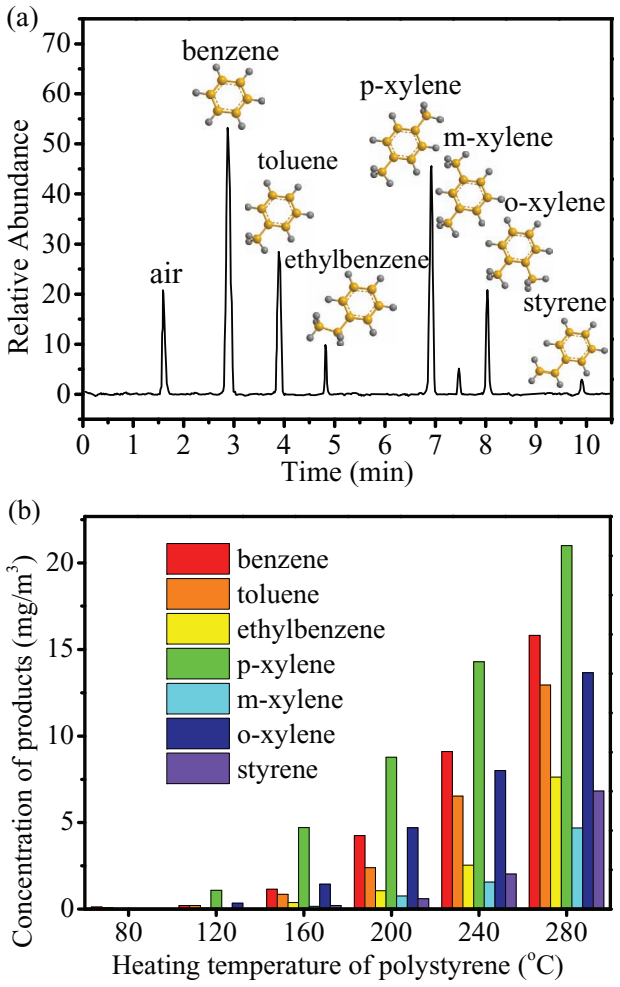

Figure 1. Investigation of polystyrene decomposition at different temperatures. a) Gas chromatography of polystyrene decomposed at 280 °C. b) Concentration of products decomposed from polystyrene at different temperatures.

spectroscopy. The results are shown in **Figure 1**a and b, respectively. From Figure 1b, it is found that polystyrene starts to decompose at about 80 °C. The product is composed of various benzene-ring containing molecules. The data is consistent to that reported in earlier literature.[11] The decomposed products are guided to the growth zone in the furnace by the carrier gases, which is a mixture of Ar/H_2. Under high temperature, they are dehydrogenated, and then connect with each other to form graphene. The schematic of CVD growth setup is depicted in Figure S1 in the Supporting Information.

To realize low nucleation density is the prerequisite for growing large single crystal graphene grains. Defects on the substrate, such as impurities, dislocation, surface irregularities normally serve as nucleation centers (see Supporting Information, Figure S2). To reduce its contribution, the copper foil was fine polished and annealed at 1050 °C in Ar/H_2 mixture for 60 minutes prior to graphene growth. The surface treatment was proven to be an important step for the controllable graphene growth, as already demonstrated by several investigations.[12,13]

Beside substrate defects, we found that H_2 flow rate also plays an important role on graphene nucleation.[14] Systematic investigations on the influence of H_2 flow rate was carried out. The growth temperature was kept at 1050 °C, and T_p maintained at 230 °C. The dependence of nucleation density on H_2 flow rate was plotted in **Figure 2**a. The nucleation density stays at a low value (around several hundred per centimeter square) when H_2 flow rate was lower than 2 sccm, it increases dramatically at higher flow rates by more than three orders of magnitude. It is necessary to mention that H_2 flow rate lower than ~2 sccm yields dendrite-shaped nucleus (as shown in the upper insert of Figure 2a) due to high anisotropic growth, while high flow rate results in hexagonal shaped nucleus (as shown in the lower insert of Figure 2a). The effects of hydrogen on nucleation density and grain shape are consistent with early observations which revealed hydrogen's double roles[15] as an activator of carbon related radicals that promotes the graphene nucleation, and as an etching reagent that controls the shape of the

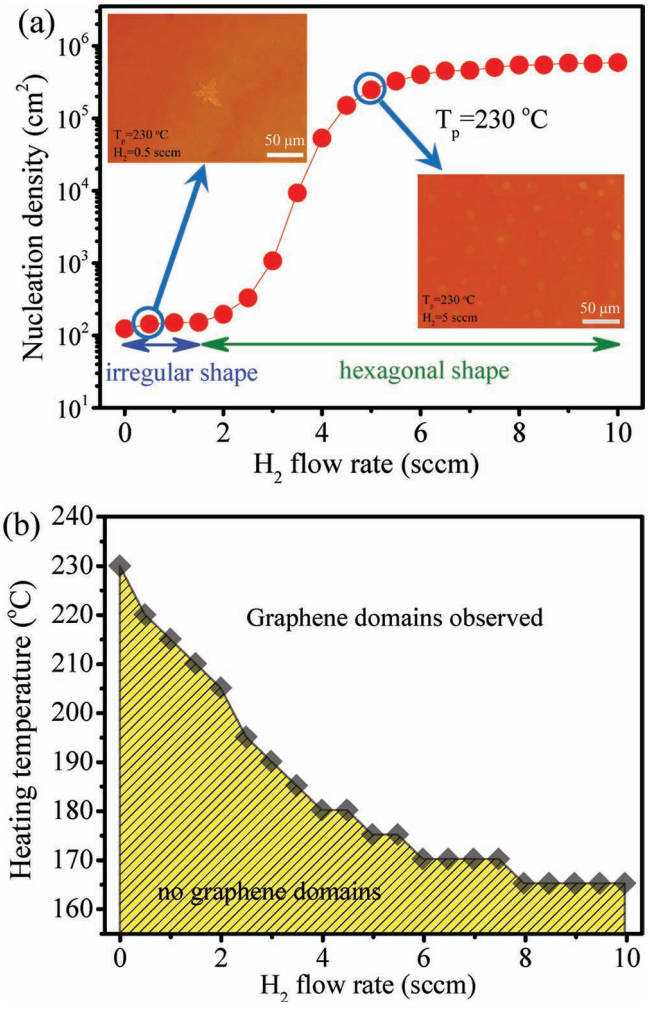

Figure 2. a) The dependence of the nucleation density on the H_2 flow rate from 0 to 10 sccm. The inserts show optical images of graphene grains synthesized under different H_2 flow rates at 1050 °C for 2 min with H_2 flow at 0.5 sccm, and 5 sccm, T_p = 230 °C. b) Critical temperature of nucleation as a function of the H_2 flow rate.

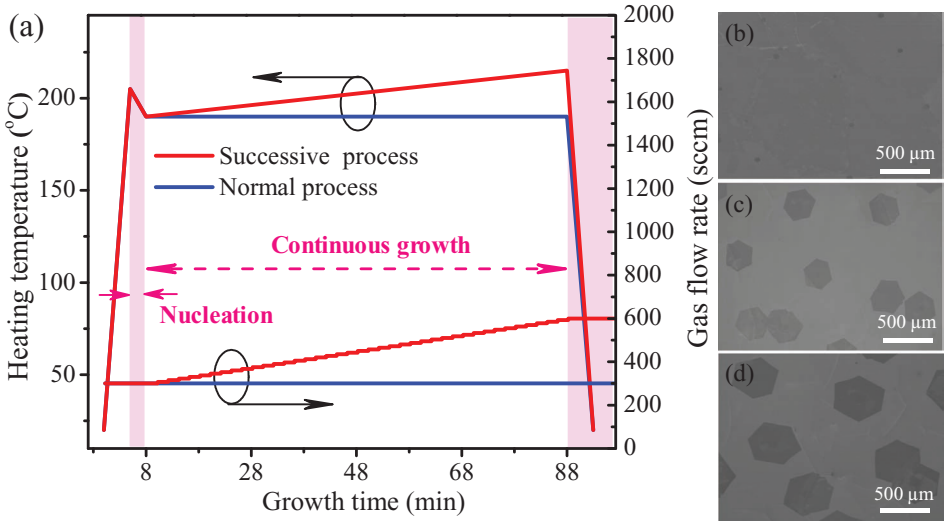

Figure 3. a) APCVD growth of graphene at 1050 °C with linear increase of T_p and total reactant gas flow rate. b) SEM image of graphene nucleation sites. c) SEM image of hexagon-shaped graphene under normal growth process for 40 min. d) SEM image of hexagon-shaped graphene under continuous growth process for 40 min.

resulting graphene grains. Proper active hydrogen radicals catalyzed on Cu foil could promote the activation of cyclobenzene related molecules by dehydrogenation effect, and the threshold of nucleation was promoted due to the supersaturation of more activated carbon related radicals on Cu foil.

In order to further optimize the behavior of graphene nucleation, we decided to examine the effect of T_p on the formation of graphene nuclei at different H_2 flow rate. Carbon supersaturation determined by T_p will certainly affects the nucleation. For graphene nucleation, it has to overcome an additional energy barrier (ΔG^*) to form crystal nucleus, accompanied by a decrease of free energy which occurs spontaneously.[16] The additional energy barrier does not exist for graphene grain growth. Nucleation threshold at different hydrogen flow rates were studied and the critical T_p at each hydrogen flow rate was obtained as shown in Figure 2b. The results suggest that a hydrogen flow rate ~2 sccm and T_p ~ 205 °C would be a very good set of process parameters for low nucleation density and control the hexagonal shape of the graphene nucleus.

From the above experiments, we developed the technology to achieve a lower nucleation density. In order to achieve large graphene grain, it is important to drive the graphene to grow at a comparatively high rate. Higher growth temperature is evidently beneficial for graphene grain growth (discussed in the Supporting Information and Figure S3). Apparently, this is due to the enhancement of the catalysis of the substrate metal at higher temperatures, which enables the higher speed of carbon construction at the edge of graphene grain. Nevertheless, the present investigations also indicate that the temperature shall not be too close to the melting point of the substrate, which will produce excessive defects in the graphene domains. According to above discussion, it should be necessary to choose a proper temperature for growth (high but not too close to the melting point of the substrate) and maintain a low H_2 flow rate (yet high enough to have sufficient etching power to control the graphene shape) to make graphene grain grow as large as possible.

Our strategy to grow the millimeter-sized graphene grain is clear. If the nuclei density is low enough, gradual increase in the supply of polystyrene is adapted to drive the continuous growth of graphene toward millimeter size. We set T_p to the critical temperature transiently to yield a low density of graphene nuclei on copper foil, and then gradually increased T_p and reactant gas flow rate to drive the continuous growth of graphene. The optimized process is shown in **Figure 3**. At the nucleation stage (as shown in the pink area in Figure 3a), the H_2 flow rate was set at 2 sccm while keeping the total flow rate at 300 sccm. T_p has to increase to a relatively high value (205 °C) to achieve supersaturation of activated carbon related molecular for initiating the nucleation (shown in Figure 3b). Once the graphene crystal nuclei were formed, T_p was decreased to below the nucleation threshold so that further nucleation was largely inhibited. During the growth stage, continuous ramping in T_p and total gas flow rate were employed. T_p increased from 195 °C to 215 °C and the total gas flow increased from 300 sccm to 600 sccm for a total time of 80 min, with the partial pressure of H_2 kept at the same value. The grain growth at increasing supply of active carbon related radicals overcomes the etching effect by H_2, resulting in a continuous growth of graphene grains. Compared to normal process (Figure 3c), larger grain size of ~500 μm was achieved after 40 min due to higher growth rate (Figure 3d). It is interesting to note that if we apply a stepwise increase of T_p, we could obtain large graphene domains with stripe-like edges (Supporting Information, Figure S4).

It was found that the growth rate of graphene grain gradually decreases with the increase of the grain size after 40 min by normal process (**Figure 4**e). Sometime, the graphene grains do not grow any more when reaction equilibrium is gradually established at the edge of graphene grains. The concentration of active carbon related radicals is not high enough to maintain the growth rate because of the reduction of the copper catalytic effect.[17] The catalytic effect degrades due to the reduction of exposed Cu surface area. To increase the

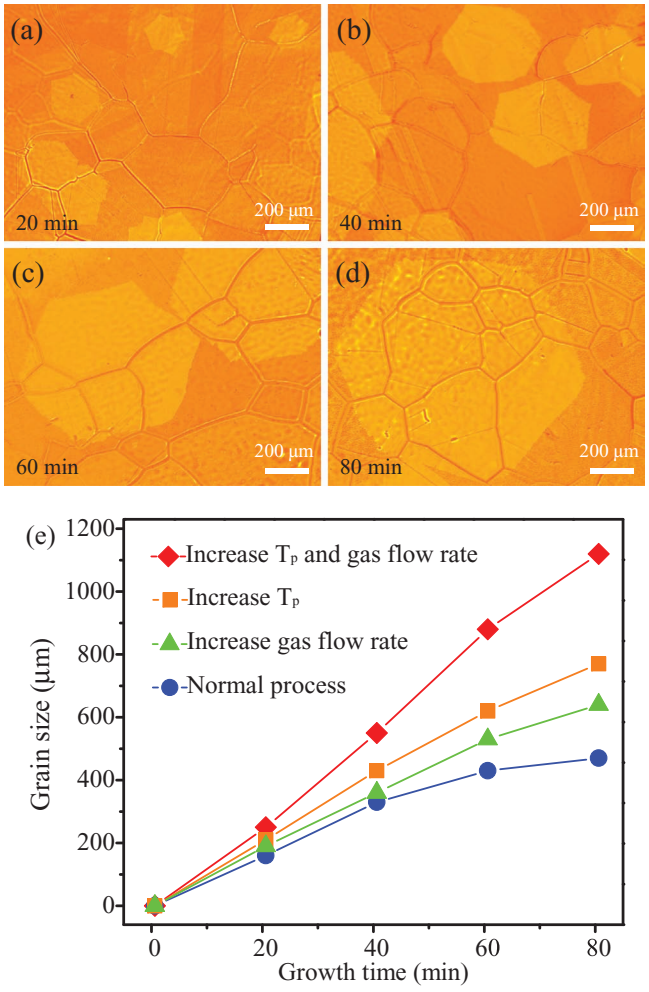

Figure 4. a–d) Optical images of hexagonal graphene grains synthesized for 20 min (a), 40 min (b), 60 min (c), and 80 min (d). The winkle-like structures in (a–d) are grain boundaries of the copper substrate. e) The grain size as a function of growth time under different processes.

grain size further, it is necessary to break the thermodynamic equilibrium of graphene growth. As shown in Figure 4e. It is clear that the process of increasing T_p and total gas flow rate can yield continuous growth of graphene grains even at 80 min. In order to find the optimal condition and to separately investigate the effect of T_p and the total gas flow rate, we conducted a series of experiments (as shown in Figure 4e). By normal process, the grain size gradually saturates at about ~420 μm at 80 min. Increasing the gas flow rate alone from 300 sccm to 600 sccm obtained the grain size to ~630 μm, while increasing T_p alone from 195 °C to 215 °C yields in a grain size of ~750 μm. If T_p and the gas flow rates are both increased, a much higher growth rate was observed, and the maximum domain size reached 1.2 mm, the biggest one reported on copper substrate. Figure 4a–d show optical images of hexagonal graphene grain synthesized in 20 min, 40 min, 60 min, 80 min, respectively. It was also found that the grain boundaries of Cu foil do not restrain the continuous growth of graphene domains. Individual hexagonal graphene grains can grow continuously across the copper grain boundaries without any apparent distortion, as shown in Figure 4a–d. This phenomenon reflects the weak influence of the Cu crystal lattice on graphene growth and demonstrates that single-crystalline graphene can grow on polycrystalline Cu foil. Figure S5 in the Supporting Information shows low magnification optical images of hexagonal millimeter-sized graphene domains transferred on SiO_2/Si substrate, from which it can be observed that large graphene grains distribute on the copper substrate quite uniform. Compared to normal process, it is clear that to gradually increase T_p and reactant gas flow rate could drive the grain grow continuously. The possible reasons are that: 1) the continuous ramping in T_p increases the concentration of active carbon related radicals on Cu foil and breaks the thermodynamic equilibrium at the graphene edges, resulting in the continuous growth of graphene grain; 2) the increase in gas flow rate also enhances the reactant feed rate and the diffusion of active carbon related radicals on the copper substrate. It also helps to remove the unwanted by-product from the Cu surface.[18] Both factors drive graphene grain toward larger size. Compared to conventional two-step process,[19] our strategy has obvious advantages in obtaining graphene in large size.

As Raman measurement could provide us the information about the number of layer and defect densities of individual hexagonal graphene domain, we conduct Raman measurement on a hexagonal graphene grain (**Figure 5**a), which was transferred onto SiO_2/Si substrate. The result was shown in Figure 5b and 5c. It is found that the full width at half maximum of 2D peak is about 28–35 cm^{-1}, the intensity ratio between 2D and G peaks (I_{2d}/I_G) is 2–3. The D peak is not observed (Figure 5d). The results indicate that most of isolated hexagon-shaped graphene grains were single layer graphene. Meanwhile, transmission electron microscopy (TEM) was introduced for crystalline structure characterizations of hexagonal millimeter-sized graphene domains (Figure 5e,f). The high-resolution TEM image (Figure 5g) indicates the graphene grain is monolayer. Selective area electron diffraction (SAED) data on different positions show the same set of hexagonal diffraction spots without rotation. It indicates that the investigated area is single crystalline (Figure 5h).

To investigate the electronic properties of hexagonal millimeter-sized graphene domains synthesized at 1050 °C, the graphene-based back-gate field-effect transistors (FETs) were fabricated on 300 nm SiO_2/Si substrates (see Supporting Information, Figure S6). A typical channel width and length were 5 μm and 10 μm. **Figure 6**a shows the typical source-drain current (I_{ds}) vs the source-drain voltage (V_{sd}) curves at different gate voltage (V_g). The linear I_{ds}–V_{ds} dependence in both cases reveals good ohmic contact between Cr/Au pads and the graphene layer. The field-effect mobility (μ) of graphene sheets can be achieved by using the following equation:

$$R_{total} = \frac{V_{sd}}{I_{sd}} = \frac{L}{W\mu\sqrt{(n_o e)^2 + (V_g - V_{diac})^2 C_g^2}} + R_c \quad (1)$$

Where R_{total} is the device resistance including the channel resistance and contact resistance R_c,[20] e is the electron charge, and n_0 is the carrier density due to residual impurities, respectively.[21] C_g is the gate capacitance per unit area

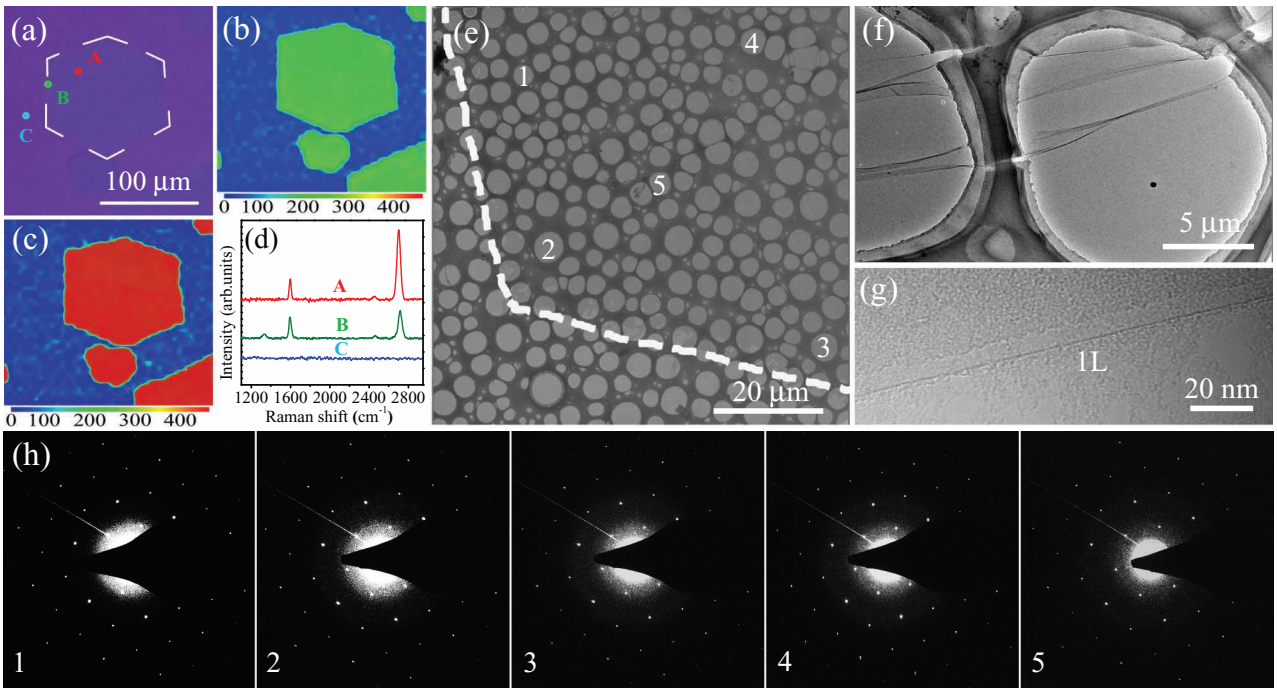

Figure 5. a) Optical image of hexagonal graphene grains on SiO_2/Si substrate. b) Intensity maps of the G bands. c) Intensity maps of the 2D bands. d) Raman spectra taken from the points indicated in (a). e) Low-magnification TEM image of a corner in hexagonal graphene grain transferred to TEM grid. f) TEM image of graphene wrinkle on the grid. g) High-resolution TEM image of monolayer graphene. h) SAED for five regions indicated as 1 to 5 in (e).

(11 nF cm^{-2}), and V_{sd} is source-drain voltage (0.1 V). L and W are channel length and width, respectively. The samples were monitored by I_{ds}–V_g curves in the measurement at room temperature. Field-effect mobility of about 5000–8000 cm^2 V^{-1} s^{-1} were obtained on 22 millimeter-sized graphene domains, suggesting that the samples synthesized by polystyrene are of high quality.

3. Conclusions

In this study, we demonstrated a simple but efficient strategy to synthesis millimeter graphene grain by controlling the supply of carbon source in chemical vapor deposition process. Polystyrene was used as a carbon source, which could provide active benzene-ring containing molecules. The nucleation density and the growth rate of graphene grain can be controlled by tuning the temperature of polystyrene and H_2 flow rates. By optimizing process parameters, nucleation density as lower as ~100 nuclei/cm^2 was achieved, and hexagonal-shaped single crystal grain up to 1.2 mm was obtained, with field-effect mobility ranging from 5000–8000 cm^2 V^{-1} s^{-1}. The Raman measurement, TEM results and electrical transport data indicate that graphene are of high quality.

With nucleation density of ~100 nuclei/cm^2, the average distance between nuclei is already in millimeter range, so in order to increase further the single crystal grain size, lower nucleation density is required which demands for further engineering efforts. Our strategy offers a high controllability of graphene growth with millimeter-size, and will definitely benefit for the practical application of graphene based electronics.

4. Experimental Section

Copper foil (Maikun Chemical 99.9%) was used as catalytic substrate. The foil was first mechanically and electrochemically polished, and then subjected to annealing at 1050 °C for 60 min in a mixture of H_2 and Ar (1:10) with gas flow rate of 300 sccm. After the pretreatment, smooth Cu surface with 0.2–2 mm large grain size could be obtained. The polishing and annealing processes are very important in reducing the vacancies, dislocations, stacking faults, phase or grain boundaries, impurity atoms and surface irregularities.[22] These processes could effectively reduce the nucleation centers. Polystyrene (Aladdin MW 100 000) was used as solid carbon source. It was loaded in a small one-side-sealed container, placed at the gas influx side of the quartz tube in the growth chamber.

The graphene synthesis was done by APCVD at a typical temperature ranging 950–1050 °C for 30–80 min. A mixture of Ar and H_2 are used as reactant gases. The H_2 flow rate was adjustable between 0–10 sccm while keeping the total flow rate at 300 sccm. Carbon supply was controlled by heating the precursor with a halogen lamp under typical polystyrene temperature (T_p) range of 80–280 °C. After the growth process, the halogen tungsten lamp was turned off, and the furnace was cooled down to room temperature naturally.

Characterizations were done by optical microscopy (Leica material Microscope DM6000M), Raman microprobe spectroscopy (Thermo Fisher DXR) using an Ar^+ laser (wavelength 532 nm) with 1 μm laser spot, equipped with an optical microscopy. Scanning electron microscopy (SEM) (FEI NOVA Nano SEM) with operating voltage of 5 kV was used for morphological investigation. Gas chromatography (Agilent 7890A-5975C) was used to investigate the products of polystyrene

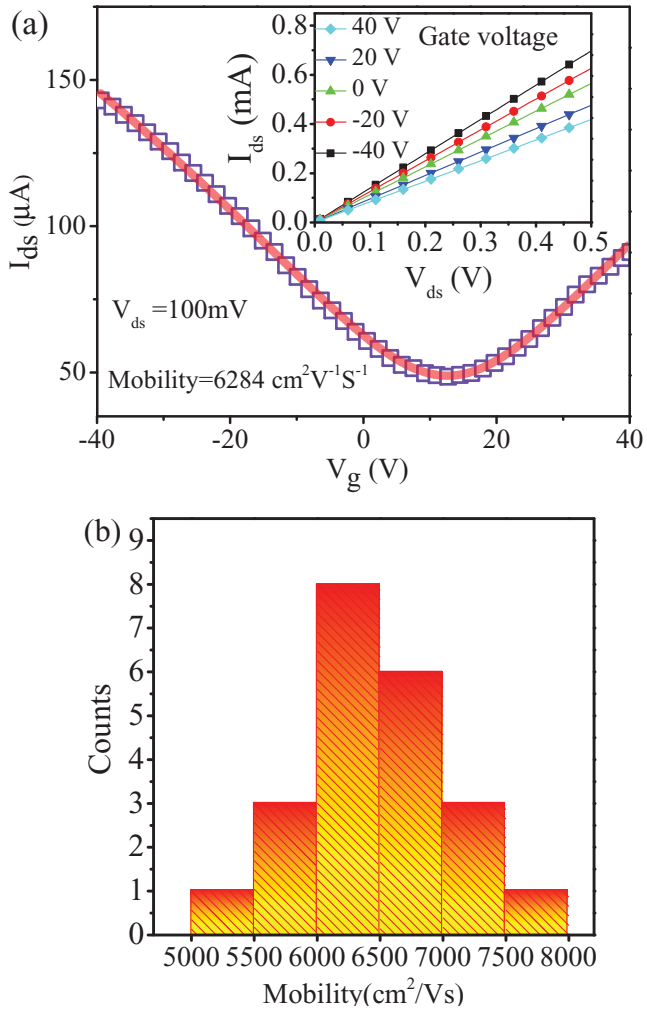

Figure 6. a) Electrical characteristics (I_{ds}–V_g) of devices at V_{ds} = 100 mV. The inset is I_{ds}–V_{ds} characteristics at various values of V_g for the graphene devices we fabricated. b) Histogram of the field-effect-mobility distribution for the total 22 devices.

during thermal decomposition. The crystalline of the hexagonal grains was characterized by transmission electron microscope (TEM, Philips CM-200 FEG, operated at 200 kV).

Supporting Information

Supporting Information is available from the Wiley Online Library or from the author.

Acknowledgements

This work was supported by projects from the National Natural Science Foundation of China (Grant No. 11104303 and 61136005), the National Science and Technology Major Project (Grant No. 2011ZX02707), Shanghai Science and Technology Commission (Grant No. 10DJ1400600) and Priority Academic Program Development of Jiangsu Higher Education Institutions.

Received: June 12, 2012
Revised: July 23, 2012
Published online: August 20, 2012

[1] A. K. Geim, *Science* **2009**, *324*, 1530.
[2] J. An, E. Voelkl, J. W. Suk, X. S. Li, C. W. Magnuson, L. F. Fu, P. Tiemeijer, M. Bischoff, B. Freitag, R. S. Ruoff, *ACS Nano* **2011**, *5*, 2433.
[3] L. Tao, J. Lee, H. Chou, M. Holt, R. S. Ruoff, D. Akinwande, *ACS Nano* **2012**, *6*, 2319.
[4] P. Y. Huang, C. S. Ruiz-Vargas, A. M. Zande, W. S. Whitney, M. P. Levendorf, J. W. Kevek, S. Garg, J. S. Alden, C. J. Hustedt, Y. Zhu, *Nature* **2011**, *469*, 389.
[5] J. An, E. Voelkl, J. W. Suk, X. S. Li, C. W. Magnuson, L. F. Fu, P. Tiemeijer, M. Bischoff, B. Freitag, R. S. Ruoff, *ACS Nano* **2011**, *5*, 2433.
[6] Q. K. Yu, A. J. Luis, W. Wei, R. Colby, J. F. Tian, Z. H. Su, H. L. Cao, Z. H. Liu, D. Pandey, D. G. Wei, *Nat. Mater.* **2011**, *10*, 443.
[7] H. Wang, G. Z. Wang, P. F. Bao, S. L. Yang, W. Zhu, X. Xie, W. J. Zhang, *J. Am. Chem. Soc.* **2012**, *134*, 3627.
[8] X. Li, C. W. Magnuson, A. Venugopal, R. M. Tromp, J. B. Hannon, E. M. Vogel, *J. Am. Chem. Soc.* **2011**, *133*, 2816.
[9] L. B. Gao, W. C. Ren, H. L. Xu, L. Jin, Z. X. Wang, T. Ma, L. P. Ma, Z. Y. Zhang, Q. Fu, L. M. Peng, *Nat. Commun.* **2012**, *3*, 699.
[10] Y. R. Luo, *Comprehensive Handbook of Chemical Bond Energies*, CRC Press, Boca Raton, FL **2007**, p. 9.
[11] F. A. Lehmann, G. M. Brauer, *Anal. Chem.* **1961**, *33*, 673.
[12] Z. T. Luo, Y. Lu, D. W. Singer, M. E. Berck, L. A. Somers, B. R. Goldsmith, A. T. Charlie Johnson, *Chem. Mater.* **2011**, *23*, 1441.
[13] G. H. Han, F. Gunes, J. J. Bae, E. S. Kim, S. J. Chae, H. J. Shin, J. Y. Choi, D. Pribat, Y. H. Lee, *Nano Lett.* **2011**, *11*, 4144.
[14] M. Losurdo, M. M. Giangregorio, P. Capezzuto, G. Bruno, *Phys. Chem. Chem. Phys.* **2011**, *13*, 20836.
[15] B. Wu, D. C. Geng, Y. L. Guo, L. P. Huang, Y. Z. Xue, J. Zheng, J. Y. Chen, G. Yu, Y. Q. Liu, L. Jiang, *Adv. Mater.* **2011**, *23*, 3522.
[16] M. Maalekian, E. Kozeschnik, *Mater. Sci. Eng. A* **2011**, *528*, 1318.
[17] X. S. Li, C. W. Magnuson, A. Venugopal, J. An, J. W. Suk, B. Y. Han, M. Borysiak, W. W. Cai, A. Velamakanni, Y. W. Zhu, *Nano Lett.* **2010**, *10*, 4328.
[18] S. Bhaviripudi, X. T. Jia, M. S. Dresselhaus, J. Kong, *Nano Lett.* **2010**, *10*, 4128.
[19] H. Bi, F. Q. Huang, W. Zhao, X. J. Lu, J. Chen, T. Q. Lin, D. Y. Wan, X. M. Xie, M. H. Jiang, *Carbon* **2012**, *50*, 2703.
[20] Y. Zhang, L. Y. Zhang, P. Kim, M. Y. Ge, Z. Li, C. W. Zhou, *Nano Lett.* **2012**, *12*, 2810.
[21] Z. Y. Zhang, Z. X. Wang, H. L. Xu, S. Wang, L. Ding, Q. S. Zeng, L. J. Yang, T. A. Pei, X. L. Liang, M. Gao, L. M. Peng, *Nano Lett.* **2010**, *10*, 2024.
[22] W. Wu, Q. K. Yu, P. Peng, Z. H. Liu, J. M. Bao, S. S. Pei, *Nanotechnology* **2012**, *23*, 035603.